PROCEEDINGS ITB Vol. 7, No. 3, 1973.

SOME NOTES ON THE DESIGN, CONSTRUCTION AND PERFORMANCE OF THE LOW-SPEED WIND-TUNNEL AT ITB

Harijono Djojodihardjo*)

R I N G K A S A N

Konstruksi dan perhitungan kerugian energi pada terowongan angin kecepatan rendah di ITB diuraikan secara garis besar.

Selanjutnya dipaparkan hasil-hasil penilaian performance dari terowongan angin ini, terutama mengenai keadaan aliran pada test-section dan hubungan antara daya input pada motor dengan kecepatan aliran pada test-section. Kecepatan angin sebesar 30 m/det dapat diperoleh pada test-section, dengan bilangan Reynolds sebesar 2 x 10^4 per cm model.

A B S T R A C T

A concise description of the design and construction of the low speed wind-tunnel at Institut Teknologi Bandung and the calculation of its energy losses are presented.

Some tests have been undertaken to evaluate its performance, in particular to evaluate the flow pattern at the test-section and the power input for a specific range of wind velocity at the test-section. The maximum velocity achieved at the test-section was 30 m/sec with corresponding Reynolds number of 2 x 10^4 per cm.

*) Mechanical Engineering Department, Bandung Institute of Technology.

I. HISTORICAL BACKGROUND

The low-speed wind-tunnel at ITB was built as a closed, single return type and powered by an automotive engine. The automotive engine drives a generator, which supplies electricity to a direct current electric motor. The electric motor drives the four bladed propeller type fan.

The initial design of the low-speed wind-tunnel at ITB was actually started in 1959 under the direction of the late Air Marshal Nurtanio (the director of what is now LIPNUR) and the assistance of ir. O. Diran. It was later assessed that the wind-tunnel would be suitable for education.

In 1962, parts of the wind-tunnel that have been constructed were presented to ITB and LAPAN (National Institute of Aeronautics and Astronautics). It was decided to build the wind-tunnel at ITB for mutual use by ITB and LAPAN, and administered by ITB. Construction of the building to house the wind-tunnel was started in 1963, and installation of the main sections was started in 1964; the project was directed by ir. O. Diran until his leave of absence from ITB at the end of 1968. In 1967 the Department of Defence and National Security (HANKAM) showed interest in assisting the project.

The financial assistance from HANKAM was realised by the end of 1968, and was partly used for completion of part of the building and installation of some additional sections.

The Department of Defence in 1969 and Department of Education (under "Pelita" Research Project) in 1970 provided research grants for the completion of the wind-tunnel construction, and the author succeeded ir. O. Diran to direct the project. Under these grants, work has been completed on the installation of the fan straightener system, the electric motor, the first cylinder and the test-section. The fourth corner turning vanes were made adjustable, and two screens were installed. Some tests were performed to evaluate the performance of the wind-tunnel with particular attention to the production of uniform flow at the test-section. With the completion of the present work, a reasonably uniform velocity of 30 m/sec and a Reynolds number of 2×10^4 per cm can be obtained at the test-section.

The present article outlines various aspects of the design and construction of the wind-tunnel, and reports some preliminary evaluation of the air flow at the test section.

II. GENERAL FEATURES OF THE WIND-TUNNEL DESIGN

A schematic diagram of the low-speed wind-tunnel at ITB is shown in figure 1. The main components of the wind-tunnel are the test-section, the first diffuser, the first cylinder, the second corner, the fan straightener system, the second

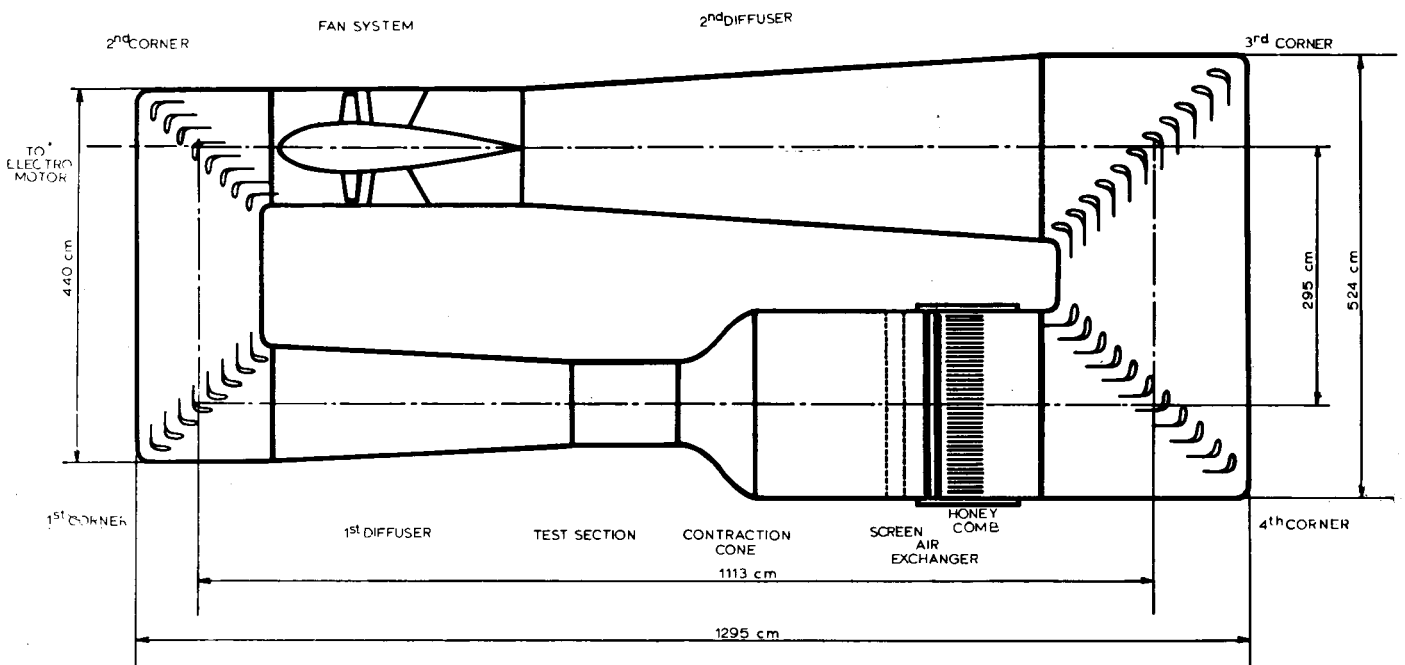

Figure 1. Schematic Diagram, Wind-Tunnel.

diffuser, the second corner, the third corner, the settling chamber with air-exchanger, honeycombs and screens, and the entrance cone. Each corner section is provided with turning vanes.

The cross section of most parts of the wind-tunnel is octagonal. The tunnel walls are built from steel plating strengthened by steel frames. The entire tunnel is placed indoor, and has a planview dimension of 12.95 m long by 5.24 m wide.

a. The Test-Section

The test-section has an octagonal cross section, with an average dimension of 1 m wide and 1 m high, or an equivalent diameter of 1.03 m. The length of the test-section is 1.30 m, and was made slightly tapered (the downstream equivalent diameter is 10 mm wider than the upstream equivalent diameter) to maintain constant pressure along the test-section. The test-section is provided with glass windows for viewing the model. The test-section is also equipped with a turntable to mount the model which can be adjusted manually. At present, due to the limitation imposed by the powerplant and the electric motor set up, a maximum velocity of 30 m/sec can be obtained at the test-section.

b. Power Losses

To calculate the power losses throughout the tunnel components, the method of Wattendorf (see ref. 1) was applied. The calculation was performed by R. Ramelan (2) to design the propeller fan and later verified by Marzwan Agus (3). The calculation procedure was to break down the tunnel into (1) cylindrical sections, (2) corners, (3) expanding sections and (4) contracting sections, and to calculate the loss for each.

The loss of energy in each section is usually written as a drop in static pressure, Δp, or as coefficient of loss, K, which is the ratio between Δp and the dynamic head q. Wattendorf refers these local losses to the jet dynamic pressure, defining the coefficient of loss as:

$$K_o = \frac{\Delta p}{q} \cdot \frac{q}{q_o} = K \frac{q}{q_o}$$

Where subscript $_o$ refers to the test-section, and $K = \frac{\Delta p}{\frac{1}{2} \rho U^2}$. With the above definition, the energy loss at each section may be referred to the jet energy. As an indica-

tion of power losses in the tunnel, the energy ratio was defined as the ratio of the jet energy at the test-section to the summation of circuit losses. Following this procedure, power losses were computed for various velocities at the test-section.

For cylindrical section, the power loss can be expressed as:

$$K_o = \lambda \left(\frac{L}{D}\right)\left(\frac{A_o}{A}\right)^2$$

Where: L - the length of the section

D - the diameter or equivalent diameter

D_o - the diameter of the test section

A_o - the area of the test-section

λ - coefficient of friction.

The friction coefficient can be evaluated following von Karman's formula:

$$\frac{1}{\sqrt{\lambda}} = 2 \log R\sqrt{\lambda} - 0.8$$

Since λ is dependent on Reynolds number, the latter should first be assumed. Note that this value of λ is valid for smooth cylindrical sections. Neglecting roughness effect, this formula was used for estimating power losses in the cylindrical sections including the test-section. For divergent sections, K_o is the summation of wall friction and expansion losses. Here:

$$K_o = \left(\frac{\lambda}{8 \tan\left(\frac{\alpha}{2}\right)} + 0.6 \tan\frac{\alpha}{2}\left(1 - \frac{D_1^4}{D_2^4}\right)\right)\frac{D_o^4}{D_1^4}$$

Where: α - the divergence angle between opposite walls

D_1 - smaller diameter

D_2 - larger diameter.

For corner sections with guide vanes:

$$K_o = \left(0.10 + \frac{4.55}{(\log R)^{2.58}}\right)\frac{D_o^4}{D^4}$$

which is partly empirical.

In the contraction cone the pressure drop is given by:

$$K_o = 0.32\ \lambda \frac{L_c}{D_o}$$

Where: λ - mean value of friction coefficient
L_c - length of the contraction section
D_o - diameter of the test-section.

Losses in the honeycomb are computed by using the following relationship:

$$K_o = K \frac{D_o^4}{D^4}$$

Where: D_o - diameter of the test-section
D - diameter of the settling chamber
K = 0.2 for honeycombs with hexagonal mesh and length to diameter ratio equal to 3.0.

Table 1 shows principal dimensions of various sections.

Table 1

Principal Dimensions of Various Sections

Section	Diameter	Length	Divergence Angle
Test-section	D_o = 1.03 m	L_o = 1.03 m	
First Diffuser	D_1 = 1.03 m D_2 = 1.42 m	L = 3.00 m	
First Cylinder	D = 1.43 m	L = 1.10 m	
Second Corner	D = 1.43 m		
Second Cylinder	D = 1.43 m	L = 1.90 m	
Second Diffuser	D_1 = 1.40 m D_2 = 2.30 m	L = 6.00 m	$\tan \alpha = 0.075$
Third Corner	D = 2.30 m		
Fourth Corner	D = 2.30 m		
Settling Chamber	D = 2.30 m	L = 3.25 m	
Contraction Cone	D_1 = 2.30 m D_o = 1.03 m	L = 1.80 m	

Losses for various velocities are tabulated in table 2. This result can be employed to estimate the amount of power required to drive the fan. It should be kept in mind that the above definition of the energy ratio excludes the losses occuring at the fan nacelle and straightener system which should be taken into account in estimating the power required to drive the fan. The above definition of the energy ratio also excludes the efficiency of the electric motor driving the fan.

Table 2

Losses at wind-tunnel components for various velocities

Test-section velocity (m/sec)	15	18	20	23	26
1. Test-Section	0.0147	0.0145	0.0143	0.0139	0.0136
2. First Diffuser	0.0468	0.0464	0.0459	0.0451	0.0444
3. First Corner	0.0394	0.0391	0.0388	0.0386	0.0383
4. First Cylinder	0.0002	0.0002	0.0002	0.0002	0.0002
5. Second Corner	0.0394	0.0391	0.0388	0.0386	0.0383
6. Second Diffuser	0.0159	0.0159	0.0158	0.0157	0.0156
7. Second Cylinder	0.0004	0.0004	0.0004	0.0004	0.0004
8. Third Corner	0.0425	0.0425	0.0424	0.0423	0.0421
9. Fourth Corner	0.0425	0.0425	0.0424	0.0423	0.0421
10. Honeycombs	0.0080	0.0080	0.0080	0.0080	0.0080
11. Screens	0.0070	0.0070	0.0070	0.0070	0.0070
12. Fourth cylinder	0.0006	0.0006	0.0006	0.0006	0.0006
13. Contraction Cone	0.0065	0.0064	0.0063	0.0062	0.0060
ΣK_o	0.2639	0.2626	0.2609	0.2589	0.2566
$1/\Sigma K_o$	3.79	3.80	3.83	3.86	3.90
30% Leakage	1.14	1.14	1.15	1.16	1.17
Energy Ratio	2.65	2.66	2.68	2.70	2.73
Jet Energy, HP	2.2	3.81	5.22	7.95	11.5(
Energy Loss, HP	0.83	1.03	1.95	2.95	4.23
Measured Input Electric Motor HP	3.38	5.00	6.85	9.78	12.20
Energy Loss/Input HP	0.246	0.206	0.285	0.302	0.347

c. Fan-Flow Straightener System

The fan is located downstream of the second corner, following the commonly accepted practice. This choice of the location of the fan was dictated by the following factors: 1) the fan develops its highest efficiency if it is located in a stream of fairly high velocity, 2) its cost is at least partially proportional to its diameter squared and 3) if the fan is to be driven by a motor outside the tunnel the corner location offers a short shaft length (1).

The fan of the present wind-tunnel is similar to a propeller of an airplane, and has four blades. Although the wind-tunnel fan seems similar to the propeller of an airplane, it operates under peculiar condition that place it in a class by itself, since the wind-tunnel fan is prevented by the law of continuity for incompressible fluid from producing an increase of velocity in the slip stream. The fan-flow straightener system employs a fan with straightener vanes behind it, without installation of prerotation vanes. For simplicity of construction, the fan blades as well as the straightener vanes are built as fixed pitched blades.

d. Fan Design

The fan diameter is 1.40 m, and the fan section has an area of 1.54 m^2. The fan boss diameter is 0.84 m, which is similar to the diameter of the nacelle. The number of the fan blades is four, while there are seven straightener vanes. Table 3 shows the design calculation results. The design fan tip speed will be 125 m/sec, which is well below the maximum allowable speed of 500 m/sec, a figure suggested to avoid excessive compressibility effects.

e. The Straightener Vanes

It has been shown (1) that satisfactory anti-twist or straightener vanes can be made by using the NASA symmetrical airfoils set with their chords parallel to the tunnel centerline provided that the amount of twist to be removed is small compared to the axial velocity. The limiting twist is that required to stall the vanes, i.e. $e = \omega r/u = \tan \tau$ (where τ = angle of twist in the slip-stream and ω = angular velocity in the slip-stream at radius r) must correspond to an angle less than α_{stall} of a symmetrical section at infinite aspect ratio including multiplane interference. The straightener vanes with constant thickness along the radius were designed, with thickness

ratio of 0.15. Table 3 also shows the dimension of the straightener vanes. The detail of the design was reported in references 2 and 3.

Table 3

Fan Blade & Straightener Vanes Design Specification*)

Ratio of radial distance from the fan axis to the fan radius / Design Variables	0.6	0.7	0.8	0.9	1.0
η_f - fan efficiency	0.953	0.952	0.951	0.950	0.949
L/D - lift to drag ratio	44.8	52.5	54.5	60.2	63.5
ϕ - advance angle	30°20'	26°17'	23°10'	20°39'	18°41'
C_s - chord of straightener vanes (m)**)	0.382	0.446	0.506	0.573	0.636
t_s - thickness of straightener vanes (m)**)	0.075	0.075	0.075	0.075	0.075
ω - slipstream rotational velocity (rad/sec)	15.02	11.04	8.45	6.67	5.41
V_T - tangential relative velocity (m/sec)	49.6	58.9	67.9	77.0	85.9
V_R - relative resultant velocity	57.5	65.6	73.8	82.4	90.8
α_o - angle of attack	1°	2°	2°48'	3°30'	4°
C - local chord length of fan blade (m)	0.195	0.158	0.125	0.103	0.093
β - geometric helix angle of fan blade	31°20'	28°17'	25°58'	24°9'	22°4'

*) from ref. 2

**) from ref. 3

f. The nacelle

Following a recommendation in ref. 1, the nacelle diameter behind the fan was chosen to be 0.6 times the diameter of the fan, i.e. 0.84 m; the nacelle has a length of 1.40. The return passage where the nacelle is located has a diffusion angle of 7°.

g. Corner vanes, honeycombs and screens

The corner vanes were made from wood; the turning angle of the fourth corner vanes can be adjusted: The honeycombs were located upstream of the fourth corner vanes, with grid size of 14 cm equivalent diameter and 40 cm long. Two screens of gauze wire 36 grids per cm^2 were installed downstream of the honeycomb.

III. SOME PERFORMANCE EVALUATION

3.1. Scope and Objectives

Having completed most parts of the design and construction, evaluation should be made on the extent to which design specification are met in order to obtain further information regarding future modifications and improvements. Since access to elaborate instrumentations is limited, the evaluation procedure involves the use of modest instrumentation, such as pitot tube and multiple manometer. The main objectives in performing the tests were:

1. to evaluate the uniformity of flow in the test-section.
2. to evaluate the performance of the wind-tunnel, in particular to determine the relationship between power and velocity.

Some modifications were also performed to obtain a reasonable degree of flow uniformity.

3.2. Test Procedure and Instrumentation

The present investigation requires only the use of pitot tube, fluid multiple manometer (which was built at the mechanical engineering workshop) and thermometer. The control desk of the wind-tunnel allows adjustment of the voltage and current of the direct current motor. The automotive engine is controlled separately to vary the horse-power supplied to the electric motor. These adjustments were made to vary the windspeed at the test-section.

During the course of the series of tests, some modifications were made. The turning vanes of the fourth corner were made adjustable, and were adjusted to obtain the desired degree of flow uniformity at the test-section. In addition two

screens were installed in succession in the settling chamber of the honeycomb.

3.3. Results and Discussion

Several readings were performed to investigate the velocity fluctuations at the test-section. Results from these tests indicate that the installation of the screens has improved the average velocity variation of the flow at the test-section from more than 2% (without the screen, with adjustment of the turning vanes at the fourth corner), to less than 1%. A typical velocity distribution at the test-section is shown in figure 2, which was obtained for electric motor horse-power of 14.5 HP and speed of 930 rpm; the corresponding average flow velocity at the test-section was 30 m/sec. It was also observed, that the velocity possesses an unsteadiness of 2%.

Figure 3 shows velocity distribution at a second station. The second station is located at 20 cm downstream of the first section, which is located halfway along the test-section. At the second station, the average velocity variation has increased to 0.76%, as compared to 0.5% at the first station. Velocity distribution at these sections suggests the presence of some secondary flow.

Table 4 shows variation of static pressure along the test-section. The indicated decrease of static pressure of less than 1% between extreme ends of the test-section can be considered satisfactory. The amount of pressure drop along

Table 4

Variation of Static Pressure Along the Test-Section
(in inches of water)

Distance from inlet section (cm)	n=900 HP=3.38	n=1000 HP=4.77	n=1100 HP=6.31	n=1200 HP=9.12	n=1300 HP=11.73
0	0.895	1.005	1.235	1.615	1.920
10	0.915	1.010	1.245	1.610	1.925
20	0.915	1.010	1.245	1.615	1.945
30	0.915	1.015	1.245	1.620	1.965
40	0.915	1.015	1.245	1.605	1.955
50	0.915	1.025	1.235	1.595	1.960
60	0.895	1.005	1.230	1.575	1.950
70	0.895	1.005	1.225	1.575	1.955

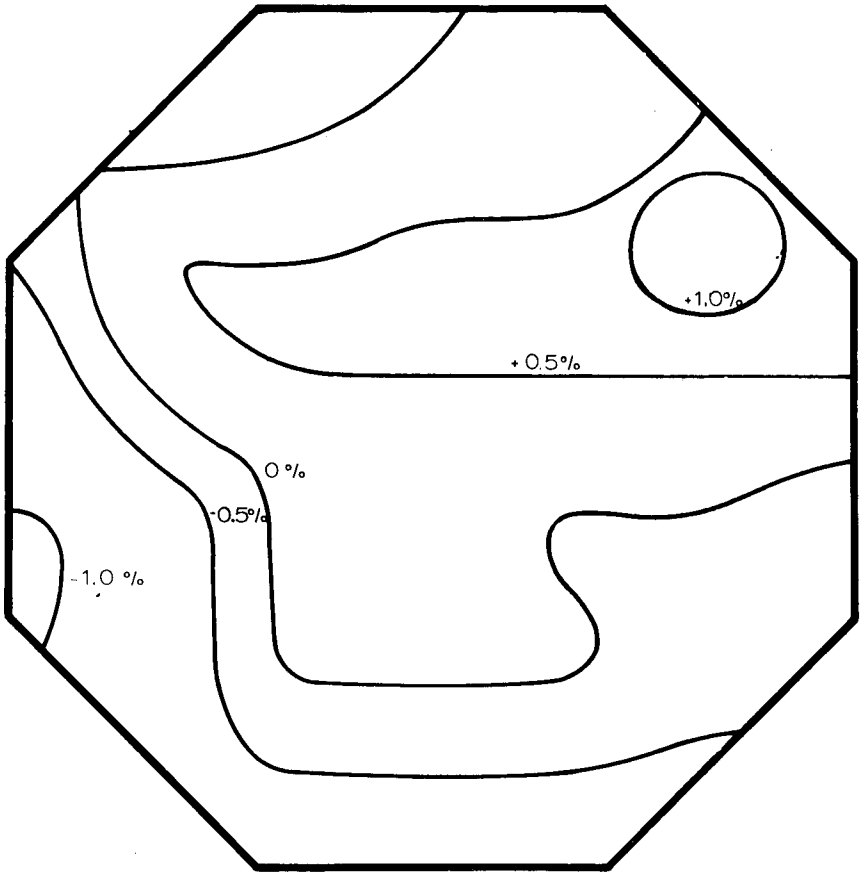

Figure 2. Velocity Contour at the Test Section measured at the center of the Test Section. Average velocity = 30.15 m/sec with standard deviation of = 0.45%.

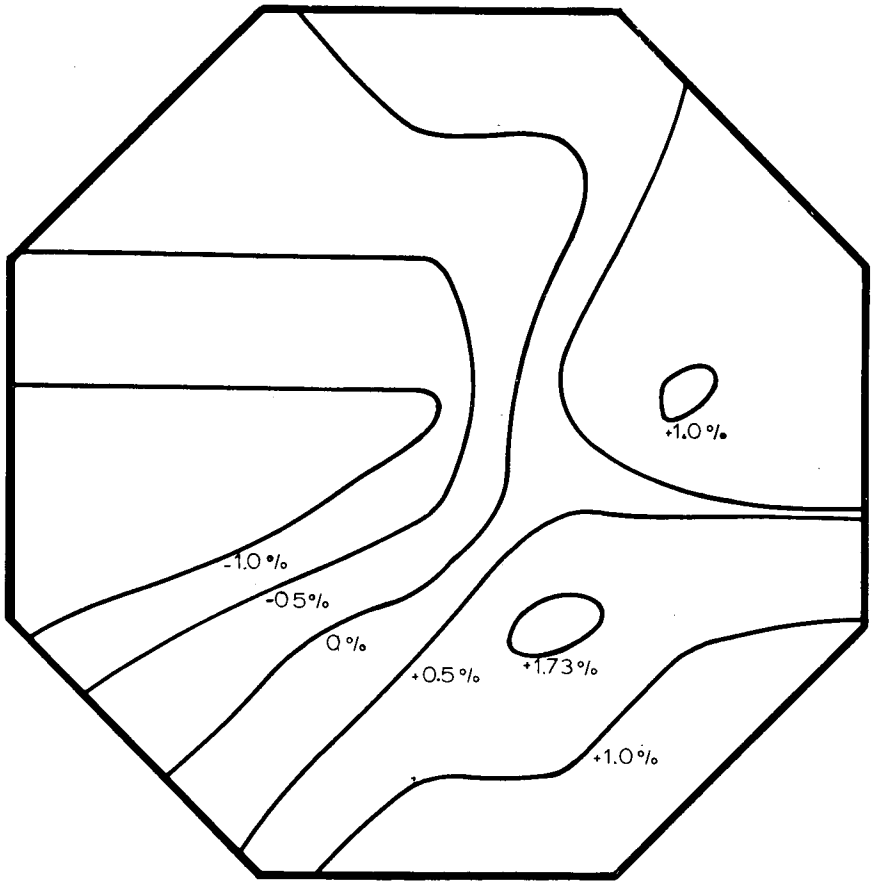

Figure 3. Velocity Contour at the Test Section, 20 cm downstream of the center Section. Average velocity 30.13 m/sec with standard deviation of 0.70%.

the test-section should be taken into consideration for correcting drag measurement. The three dimensional extent of the flow should be investigated further by using a yaw probe.

The variation of electric motor horse-power to wind-speed at the test-section is shown in figure 4, which also describes calculated estimation as tabulated in table 2. Discrepancy with calculated estimation is considerable. This discrepancy should be subject to further work, but some remarks are in order.

Part of this discrepancy may be due to inaccuracies in estimating the energy ratio, which also indicates the discrepancies between estimated loss-factor and true loss-factor at wind-tunnel components. Losses occuring at the corner section with stationary turning vanes can be larger than estimated if the vanes were improperly positioned during installation. However most of this discrepancy is believed to be due to unfavourable flow entering the fan (since the entrance nacelle upstream of the fan is not smooth), lower efficiency of the fan at off design condition and losses in the electric motor.

The performance of the present propeller fan should be evaluated before performing any modification to increase the capabilities of the fan. Originally it was designed to obtain a velocity of 40 m/sec in the test-section (2). However at present only a maximum velocity of 30 m/sec was obtained.

This situation is believed to be partly due to the limitations imposed by the combustion engine and the generator, and partly due to the off design flow situations upstream of the fan. The power plant set up was assembled by using second hand engine, generator and electric motor. Although each of them has been repaired and reconditioned, their capabilities, are still limited. The combustion engine employed in the present set up is a 1948 model of truck engine made by Chrysler corporation. The electric motor is capable of delivering no more than 28 HP to the fan shaft. The propeller fan was designed by a staff member at the Mechanical Engineering Department (2) and manufactured locally.

IV. CONCLUSIONS AND RECOMMENDATIONS

The following conclusions can be drawn:

1. The development of the low-speed wind-tunnel at ITB has reached a stage where a reasonably uniform velocity for educational purposes can now be obtained at the test-section. The mean velocity at the test-section was less than 1%, while unsteadiness has been reduced to about 2%. The frequency of the unsteadiness was about 30 cycles per minute at test-section velocity of 26 m/sec.

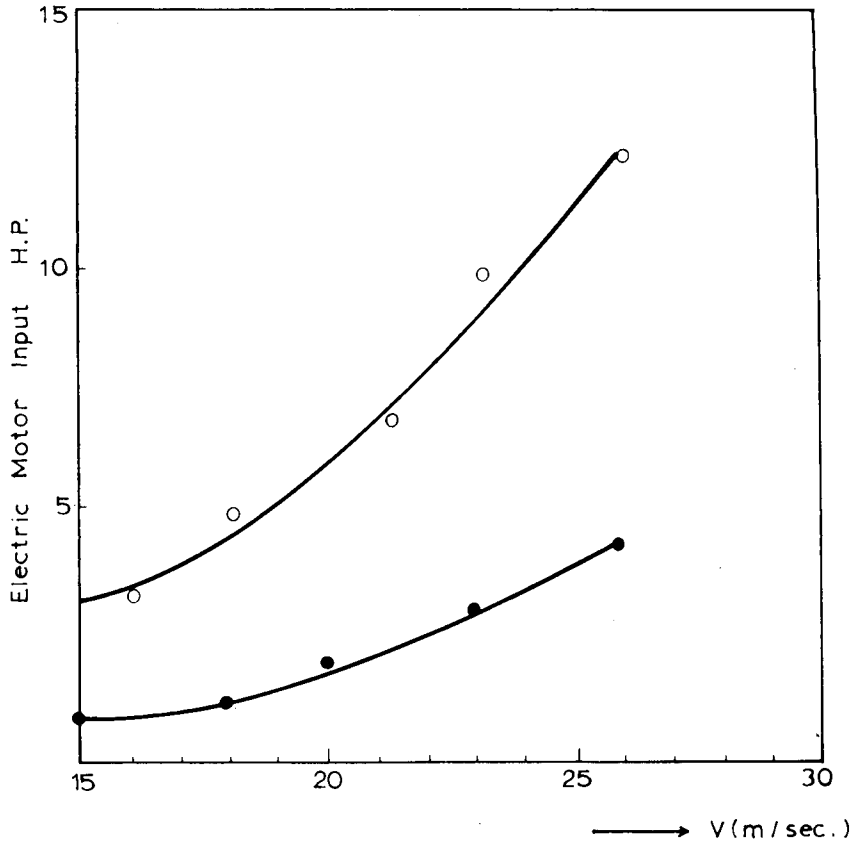

Figure 4. Power-Velocity relation

2. The maximum velocity obtained at the empty test-section with the present power plant was 30 m/sec.
3. The static pressure variation along the tunnel was within 2% of the mean static pressure.

The following are recommended for future work:

1. Several tests should be made to evaluate the performance of the propeller fan and to perform some modification.
2. Further test should be conducted to evaluate and reduce secondary flow effects. Particular attention should be focussed on the flow along fan-straightener vanes system.
3. Effort should be made to reduce flow unsteadiness at the test-sections, possibly by introducing additional honeycombs at the expense of additional power losses.
4. Turbulence and boundary layer measurement should also be performed in the near future.

V. ACKNOWLEDGEMENT

The author would like to acknowledge ir. O. Diran for providing useful informations. Mr. Marzwan Agus has assisted the author in performing some of the tests and modification of the wind-tunnel sections, while Mr. Roediono K. Djatikoesoemo has assisted the author in calibrating the flow at the test-section.

VI. REFERENCES

1. Alan Pope: "Low-Speed Wind-Tunnel Testing", John Wiley & Sons Inc., 1968.
2. Roedianto Ramelan: "Design of a Fan-Straightener System for the ITB Subsonic Wind-Tunnel", unpublished report, Mechanical Engineering Department, ITB, 1968.
3. Marzwan Agus: "Evaluation of the Performance of the Wind-Tunnel", Mechanical Engineer Thesis, Department of Mechanical Engineering ITB, 1972 (in Indonesian).

(Received 22nd June 1973)